

Dynamically Induced Thermal Stresses in Composite Material, Structural Panels

A. R. Zak*

University of Illinois, Champaign-Urbana, Ill.

and

W. H. Drysdale†

U.S.A. Ballistics Research Laboratories, Aberdeen Proving Ground, Md.

It is shown that appreciable thermal stresses can be produced in a structural panel made of a composite material when such a model is subject to dynamic loads. The mechanism for this phenomenon is the viscous damping, which has been shown to exist in certain fiber-reinforced composite materials. In the present analysis, the loading is provided by assuming that the panel is subject to a high intensity sound pressure level, which could occur in certain practical situations. The amount of damping used corresponds to previously measured values of loss factor in real materials. The damping causes energy dissipation, some of which is transferred to the surrounding medium, and the remainder acts to raise the temperature of the panel. This temperature increase is shown to produce compressive thermal stresses, which can be sufficient to cause structural instability. This is illustrated by calculating the effect of these stresses on the fundamental frequency of the panel. The analysis is formulated in terms of finite elements and numerical results are presented.

Nomenclature

A	= area of a rectangular element
$c_1 - c_{12}$	= coefficients in displacement functions
E	= uniaxial modulus
F	= force matrix for the panel
f_j	= modal force for a rectangular element
G	= shear modulus
g_j	= loss factor for j th mode
i	= imaginary part
K	= stiffness matrix for a panel
K', K''	= real and imaginary parts of K
k	= heat conduction of air
k'_{jk}, k''_{jk}	= real and imaginary parts of stiffness coefficients for an element
L	= length of the panel
M	= mass matrix for the panel
m_{jk}	= mass coefficients for an element
N_{Pr}	= Prandtl number
N_{Re}	= Reynolds number
P_j	= amplitude of harmonic pressure at frequency ω_j
Q	= displacement vector for the panel
Q', Q''	= real and imaginary parts of Q
q	= displacement vector for an element
q', q''	= real and imaginary parts of q
q_j	= nodal displacement of an element
q'_j, q''_j	= real and imaginary parts of q_j
R	= rate of energy dissipation in an element
R_j	= rate of energy dissipation in an element by the j th mode
Re	= real part of complex quantity
SPL	= sound pressure level
$S(\omega)$	= power spectral density
t	= time
u, v	= in-plane displacements of the panel
w	= transverse displacement of the panel
W	= energy dissipation in an element over one load cycle

W_j	= energy dissipation in an element over one load cycle by the j th nodal force
x, y	= in-plane coordinates of the panel
α	= coefficient of thermal expansion of the panel
μ	= kinematic viscosity of air
ν	= Poisson's ratio
ω	= frequency
ω_j	= natural frequency of j th mode
ρ	= density of panel per unit area
σ_{xT}, σ_{yT}	= in-plane thermal stresses
θ	= temperature increase in an element

Introduction

PREVIOUSLY published experimental results¹⁻³ have shown that certain fiber-reinforced material exhibit measurable amounts of viscous damping. These results are consistent with prior tests⁴ on epoxy resin materials in which strong viscoelastic behavior has been observed. Such properties certainly would be transferred to composite materials when these resins are used as the matrix for the fibers. Previous tests in this area have been conducted under sinusoidal dynamic loading conditions, and under these conditions, the viscoelastic response is characterized by the storage and the loss moduli. Available data indicate that the loss modulus is only a few percent of the storage modulus. Consequently, in many practical applications, such as, for example, low frequency or dynamic loads of short duration, the effect of viscous damping is negligible. However, other situations can be envisaged in which such material damping can have appreciable effect on structural response. One such effect is the temperature increase when the material is subjected to sinusoidal loading.¹ The intent of the present analysis is to examine the effect of such temperature rise on the dynamic response of flat structural panels. This effect will be in a form of compressive, in-plane stresses, which will act to reduce the effective bending stiffness of the panels.

The analysis will be concerned with laminated rectangular panels possessing realistic composite material properties. The dynamic loading conditions will be provided by assuming that the panel is subject to a high intensity, broad band, noise. The pressure level in the noise will be chosen to simulate practical situations arising from a jet propulsion system. Theoretically, under these loading conditions, the panel will respond with

Received July 19, 1974; revision received July 17, 1975.

Index categories: Structural Composite Materials; Structural Dynamic Analysis; Thermal Stresses.

*Professor, Aeronautical and Astronautical Engineering Dept. Member AIAA.

†Research Engineer.

most of its natural frequencies; however, in the present analysis, the response will be considered to be composed of a finite number of frequencies and corresponding mode shapes. In order to consider the dynamic response as characterized by natural frequencies we shall make use of certain statistical energy ideas developed for the analysis of single resonators subject to broad-band excitation.⁵

The solution for the structural response will be performed numerically, using two different finite-element models. One model will be used to examine the dynamic bending response and the resulting energy dissipation, and the second model will be used to evaluate the thermal stresses.

Harmonic Response

The present analysis will be applied to laminated, rectangular flat panels shown in Fig. 1. The individual layers of the orthotropic material will be assumed to be symmetrically distributed relative to the middle surface. This arrangement will permit uncoupling between the bending and the stretching deformation. The dynamic motion of the panel will be assumed to be in the bending mode. The excitation will be provided by a uniformly distributed, broad band pressure load. The first step in analyzing the response to broad frequency excitation is to consider the response to the harmonic loading.

The harmonic response of the panel will be obtained numerically, by use of a finite-element formulation. Because of the geometrical symmetry it is sufficient to consider only one quadrant of the panel, and this region is divided into sixteen rectangular elements, as shown in Fig. 1. In order to apply the finite-element method to viscoelastic materials, use is made of previously developed⁶ elastic-viscoelastic analogy. This analogy states that the governing equations for a viscoelastic structure, subject to harmonic excitation, have the same form as a corresponding elastic problem with the elastic material properties being replaced by the corresponding complex, dynamic quantities. This implies that the elastic finite-element method formulation can be used as the starting point for the present analysis.

The finite-element model used in this analysis is based on the following displacement variation over the element

$$w = c_1 + c_2x + c_3y + c_4x^2 + c_5xy + c_6y^2 + c_7x^3 + c_8x^2y + c_9xy^2 + c_{10}x^3 + c_{11}x^3y + c_{12}xy^3 \quad (1)$$

The displacement variation given by Eq. (1) has been used previously for elastic, flat-plate problems, and the corresponding mass and stiffness matrices can be found in the literature.⁷ In the present situation, the individual stiffness matrices and mass matrices are identical, and they can be combined to obtain the governing equations for the total panel. For harmonic excitation with frequency ω , these equations have the matrix form

$$-\omega^2 [M] \{Q\} + [K] \{Q\} = \{F\} \quad (2)$$

By use of the previously mentioned analogy,⁶ Eq. (2) can be applied to viscoelastic panel by replacing the elastic stiffness matrix by a corresponding complex matrix defined by

$$[K] = [K'] + i [K''] \quad (3)$$

The displacement matrix in Eq. (2) represents the amplitude of the harmonic response, and in general it will be a set of complex numbers, which can be represented by

$$\{Q\} = \{Q'\} + i \{Q''\} \quad (4)$$

By use of Eqs. (2-4) it is possible to solve for the real and imaginary parts of the displacement vectors, and these

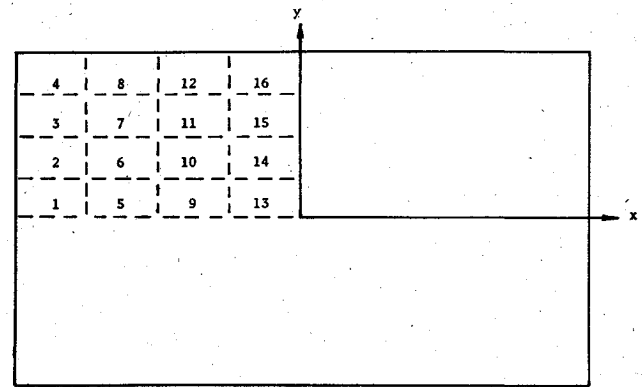


Fig. 1 Finite element grid used to represent one quadrant of the rectangular panel.

solutions can be shown to be

$$\begin{aligned} \{Q''\} &= [-K'' - (-\omega^2 M + K) [K'']^{-1} [-\omega^2 m + K']]^{-1} \\ \{F\} \times \{Q'\} &= -[K'']^{-1} [-\omega^2 m + K'] \{Q''\} \end{aligned} \quad (5)$$

From Eqs. (5), the nodal displacement q can be obtained for each individual element.

Energy Dissipation

The energy dissipation in the panel due to the harmonic loading is calculated using the results from Eqs. (5). In order to calculate the spatial temperature distribution, the dissipation is calculated for each element by analyzing the work done over one cycle of load. This is found by considering work done by a general nodal force f_j over one period of vibration

$$W_j = \int_0^{2\pi/\omega} \text{Re}(f_j) \text{Re}\left(\frac{dq_j}{dt}\right) dt \quad (6)$$

By use of the relation between nodal forces and displacements, and summing Eq. (6) over the 12 degrees-of-freedom, the total dissipation from an element is obtained in the following form

$$\begin{aligned} W &= \pi \sum_j \sum_k [\omega^2 m_{jk} (q_j' q_k'' - q_j'' q_k') \\ &\quad + k_{jk}' (-q_j' q_k'' + q_j'' q_k') + k_{jk}'' (q_j'' q_k'' + q_j' q_k')] \end{aligned} \quad (7)$$

By making use of the dynamic equations for the element, Eq. (7) can be reduced to

$$W = \pi \sum_j \sum_k k_{jk}'' (q_j'' q_k'' + q_j' q_k') \quad (8)$$

Having the expression for the total dissipation, given by Eq. (8), it is possible to estimate the average temperature increase in the element over one load cycle. However, before doing this, the response of the panel to broad-band excitation will be considered.

Broad-Band Excitation

In order to calculate the response of the panel to broad-band excitations, use is made of certain statistical energy results previously developed for the purpose of analyzing the dynamic response of simple resonators.⁵ These results can be extended directly to the analysis of a panel structure if the damping is small, as it is in the present problem. Under the conditions of small damping it is possible to neglect modal

coupling, and consider the response of the panel to be composed of a set of linear resonators corresponding to the natural modes of the analysis.⁵ In this approach, the broad-band excitation is replaced by an equivalent set of discrete harmonic forces acting at the natural frequencies of the system. The response of each of these harmonic forces can be obtained by the analysis described in the previous section.

Consider a set of linear resonators subject to a broad-band excitation characterized by the power spectrum density $S(\omega)$. For a lightly damped system, it can be shown that this excitation is equivalent to a set of discrete forces acting at the natural frequencies of the system.⁵ In the case of the present model, which is subjected to transverse pressure loading, these discrete forces are replaced by harmonic components of pressure P_j at frequency ω_j

$$\frac{1}{2}P_j^2 = (\pi/2)S(\omega_j)g_j\omega_j \quad (9)$$

If the power spectrum density of the load is specified, P_j can be calculated from Eq. (9) and then Eqs. (5) can be used to find the panel response. If the panel response is known, the rate of dissipation is calculated from Eq. (8) by multiplying the work done per cycle by the frequency

$$R_j = (\omega_j/2\pi) W \quad (10)$$

It can be shown⁵ that the total dissipation due to the presence of broad-band excitation can be obtained by summing Eq. (10) over all of the natural frequencies

$$R = \sum_j \frac{\omega_j}{2\pi} W \quad (11)$$

There is a question of how many terms should be included in the series of Eq. (11). Theoretically, a panel model possesses infinite degrees of freedom; however, numerical data will be presented later to show that only the first few lowest natural modes contribute significantly to the dissipative process, and, consequently, the series in Eq. (11) can be relatively short.

Temperature Calculation

The first step in the temperature calculation is to evaluate the natural frequencies for the elastic panel. After the frequencies are determined, the viscoelastic response is found from Eq. (5). From these results the rate of dissipation is calculated in each finite element by use of Eq. (11). All of these steps are carried out numerically and have been programmed for computer calculations.

When the total rate of power dissipation is found in each element, the next step is to set up a steady-state heat balance equation. This balance equation calculates the element temperature after a equilibrium has been established between heat rate generation and heat removal from the panel by transfer to the surrounding medium. In the present analysis, it is assumed that the panel is relatively thin, so that it is possible to neglect heat conduction in the plane of the panel, and also that, in the thickness direction, the temperature is constant. The omission of the heat conduction in the $x-y$ plane will be conservative in the sense that it will lead to slightly higher thermal stresses. Under these assumptions, the heat balance equation is relatively simple, and can be expressed as follows

$$R = h A \theta \quad (12)$$

Equation (12) is used to calculate the steady-state temperature rise θ if the parameters R , A , and h are specified. All of the parameters in Eq. (12) are known if the heat-transfer coefficient h can be specified. In the absence of experimental data for this particular configuration, use will be made of a suitable empirical relation to calculate h .

Thermal Stress Analysis

When the temperature in each element has been established, it is possible to calculate in-plane thermal stresses. In the present analysis this is done in a separate finite-element computer program designed for plane stress problems. In this analysis the same rectangular finite element grid is used as that in the case of the vibration analysis. In this model, however, each element is divided into four triangular elements, with one apex at the center of the rectangular element. Each triangular element possess six degrees-of-freedom, and the two in-plane displacements are characterized by linear functions

$$u = c_1 + c_2x + c_3y \quad v = c_4 + c_5x + c_6y \quad (13)$$

The stiffness matrices for the triangular elements are combined to form the basic, elastic equilibrium for the rectangular elements, and then these are used to form the matrix equations for the total panel.

In the dynamic analysis, a constant temperature is calculated for each element. One approach is to use this temperature directly in the thermal stress analysis; however, it is more realistic to assume a continuously varying temperature. Consequently, the calculated temperature is applied to the center of each element, and then the temperature is extrapolated to the nodal points. The nodal temperatures are used as the input for the thermal stress calculations.

The effect of the thermal stresses in the present model is to produce nonuniform, in-plane compressive loads. When these loads become large enough, elastic panel buckling can occur. However, even before buckling actually happens, the effect of these in-plane forces can be observed on the dynamic response of the panel. The effect of the in-plane forces on the transverse vibration can be expressed in terms of a modified stiffness matrix. When these loads are compressive, the effect stiffness matrix in Eq. (2) will be reduced. It is possible to modify the finite-element program⁷ to account for this phenomena and calculate the effect of the thermal loads in terms of changes in the natural frequencies of the system.

Numerical Example

The present analysis is applied to a specific example consisting of a panel 12×7 in. on its side and 0.08 in. thick. The panel is simply supported along its edges and restrained against motion in the $x-y$ plane. The material properties for the laminated panel have been chosen to correspond to so-called "isotropic laminate," which is characterized by equal properties in the two orthotropic directions.⁸ Such a situation could be obtained by suitable arrangement of orthotropic plies, for example, using fiber orientations of $+30^\circ$, -30° , 90° , -90° , -30° , 30° with respect to $x-y$ coordinates. The present analysis, however is not limited to this arrangement, and the associated computer programs could be used for other situations as long as the plies are symmetrically arranged relative to the middle surface.

When deciding on the material properties to be used in this example, a number of previous experimental results were examined. As far as the elastic properties for fiberglass composites are concerned, there are a great deal of data available on the basis of which a reasonable set of values can be chosen. The choice of the loss moduli is somewhat more complicated, since not as many data for viscoelastic properties are available. However, since the main objective in the present analysis is to examine the thermal stress effects, it is possible to make a choice for the loss moduli which would correspond to experimentally observed energy dissipation rates. In a previous study,¹ it was observed that, for isotropic laminates, the specific energy loss per cycle of load is about 3%. The specific energy loss is defined as the ratio of the energy dissipated per cycle to the maximum stored energy. It can be shown that for materials with the same loss factor for each

modulus the specific energy loss is directly proportional to the loss factor. Consequently, for the present example a loss factor of 3% was used, and the resulting complex moduli were chosen as $E = 3.95 \times 10^6 (1 + .03i)$ psi, $G = 1.55 \times 10^6 (1 + .03i)$ psi, and $\nu = 0.275$. Other necessary physical properties used were $\rho = 0.079$ lb/in.³, and $\alpha = 0.1156 \times 10^{-4}$ in./in./°F.

Using a constant loss factor in both the uniaxial and the shear moduli leads to the result that the two parts of the complex stiffness matrix Eq. (2) are related by $[K''] = 0.03 [K']$. This can be shown from the analytical expression for the stiffness matrix of individual elements, which always contain linear terms in E and G .

To obtain characteristic values for a practical random pressure field exciting the panel, measured overall sound pressure levels (SPL) at various points of a VAK 191 B Italian VTOL aircraft in a takeoff configuration were used.⁹ The maximum value of 163 dB occurred on the underside of the wing flap. A third octave band SPL at this position indicated a relatively flat response up to 10,000 rad/sec. Since the major structural response would occur at frequencies less than 10,000 rad/sec, it is assumed in these calculations that the spectral density is constant over the range 0–10⁴ rad/sec and that the overall SPL is contained in this range. Thus, the maximum spectral density is 0.167×10^{-4} (psi)²/rad/sec.

A heat-transfer coefficient for a panel consistent with the physical situation on the bottom of a VTOL aircraft in takeoff configuration is not available. The flow would be highly turbulent, because of the reflection of the jets from the ground, but the overall flow velocity would be small. The approximate formula for the heat transfer from a plate with turbulent boundary layer over its entire surface is¹⁰

$$h = (k/L) [0.036 (N_{Re})^{0.8} (N_{Pr})^{1/3}] \quad (14)$$

where, for this example,

$$k = 0.016 \text{ Btu/hr ft}^2/\text{°F} \quad L = 1 \text{ ft}$$

$$N_{Re} = UL/\mu = 81,230 \quad N_{Pr} = 0.7 \quad \mu = 0.65 \text{ ft}^2/\text{hr}$$

A mean film temperature (average of surface and air temperature) of 100°F was assumed to obtain the properties of air, and a mean flow velocity of 14.67 fps was used to calculate Reynolds's number; by use of the preceding parameters, the following value of h was obtained: $h = 0.0745$ in. lb/sec in.²/°F. Since only an experimentally determined coefficient could be considered completely accurate for this rather complex flowfield, results to be presented have been obtained for a range of heat-transfer coefficients in the neighborhood of the previous value of h .

In general the analysis cannot be performed in one step since the thermal stresses affect the dynamic problem by changing the effective bending stiffness. Consequently, for a given set of input parameters, a number of iterations are necessary in order to obtain the equilibrium conditions. The first step of this iteration involves calculating the dynamic panel properties without the effect of the in-plane thermal stresses. These dynamic properties then are used to evaluate the dissipation and the temperature changes in each finite element. Once the temperature distribution has been established, the static finite element program is used to evaluate the thermal stresses. These stresses are used to modify the bending stiffness matrix, and the previous calculations are repeated using the new stiffness matrix. The convergence to the equilibrium conditions is governed by the choice of the initial values of the parameters h and SPL, as will be discussed later.

The analysis uses a finite number of natural modes and frequencies to characterize the response to broad-band excitation. In order to determine how many of these modes should be included, a comparative study was performed to

Table 1 Contribution of natural modes to dissipation in center element 13 (SPL = 0.15×10^{-4})

Mode number	Natural frequency, rad/sec	Energy dissipation, in.-lb/sec
1	890	3.09
2	2679.	0.19
3	6202.	0.25
4	6325.	0.03
5	7545.	0.01

Table 2 Temperature changes and thermal stresses in the panel (SPL = 0.14×10^{-4} $h = 0.0745$)

Element number	Change in temperature, °F	Initial thermal stresses, psi	
		σ_{XT}	σ_{YT}
1	3.78	-733	-362
2	6.34	-806	-514
3	9.94	-825	-668
4	12.5	-848	-812
5	13.6	-934	-725
6	11.9	-869	-738
7	11.3	-799	-771
8	9.65	-693	-791
9	23.9	-1206	-969
10	17.9	-972	-954
11	12.9	-751	-927
12	6.88	-544	-910
13	33.8	-1421	-1267
14	23.5	-1047	-1173
15	14.3	-718	-1052
16	4.02	-402	-944

examine the relative effect of various modes on the dissipation process. Table 1 shows a set of typical data for the element number 13.

The data shown in Table 1 indicates the relative contribution of the first five natural modes to the energy dissipation. It can be seen that only a small error in the total dissipated energy occurs from ignoring higher modes because of the rapid decrease in magnitude of the dissipation with the mode number. Consequently, it was decided to use only the first five modes and frequencies in all the calculations.

The numerical analysis of this particular panel was performed using a range of parameters h and SPL. The results of these calculations are summarized in the curves of Fig. 2, where the effect of SPL on the fundamental frequency is shown for different values of h . It can be seen that, for a given value of h , there is a maximum value of SPL above which the panel will buckle, as evidenced by the fundamental frequency

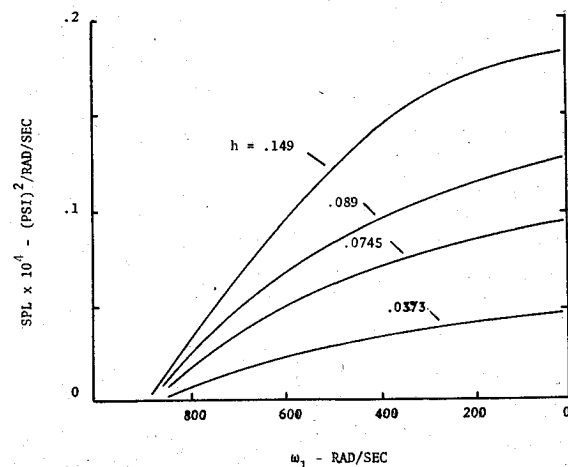


Fig. 2 Effect of spectral density level and the magnitude of heat transfer coefficient on the fundamental frequency.

going zero. For example, for $h=0.0745$ the critical value of SPL is about 0.9×10^{-5} .

In generating the data shown in Fig. 2 the iteration process described previously was employed. When the SPL was below the critical value it usually took two or three iteration cycles to obtain steady-state conditions. Above the maximum value of SPL, the second cycle of iteration would yield a negative value of frequency, indicating that the panel was buckled by initial thermal stresses. An example of such data is shown in Table 2, where the numerical results from the first iteration cycle are presented for $SPL=0.14 \times 10^{-4}$ and $h=0.0745$.

The results in Table 2 show the initial change of temperature and in-plane thermal stresses for the 16 finite-elements in one quadrant of the panel. It may be noted that the temperature changes are quite modest, but the thermal stresses that are generated were found to be sufficient to cause buckling.

Conclusions

The results of the present analysis show that even a small amount of viscous damping in composite materials can produce important thermal loads in a flat panel structure. The loads are produced by the temperature rise due to energy dissipation when the panel is subject to dynamic excitation by high-intensity sound pressure level. The temperature changes in the panel are relatively small, but they are sufficient to produce appreciable in-plane compressive stresses. Under certain conditions, these stresses are large enough to cause elastic buckling. However, even if the buckling loads are not ex-

ceeded, the compressive stresses are sufficient to cause major changes in the dynamic response of the panel as measured by the changes in the fundamental natural frequency.

References

- ¹Dally, J. W. and Broutman, L. J., "Frequency Effects on the Fatigue of Glass Reinforced Plastics," *Journal of Composite Materials*, Vol. 1, Oct. 1967, p. 424.
- ²Schultz, A. B. and Tsai, S. W., "Dynamic Moduli and Damping Ratios in Fiber-Reinforced Composites," *Journal of Composite Materials*, Vol. 2, July 1968, p. 368.
- ³Schultz, A. B. and Tsai, S. W., "Measurements of Complex Dynamic Moduli for Laminated Fiber-Reinforced Composites," *Journal of Composite Materials*, Vol. 3, July 1969, p. 434.
- ⁴Kaelble, D. H., "Dynamic and Tensile Properties of Epoxy Resins," *Journal of Applied Polymer Science*, Vol. 9, 1965, p. 1213.
- ⁵Smith, P. W. and Lyon, R. H., "Sound and Structural Vibration," NASA CR-160, April 1965.
- ⁶Hilton, H. H. and Russell, H. G., "An Extension of Alfrey's Analogy to Thermal Stress Problems in Temperature Dependent Linear Viscoelastic Media," *Journal of Mechanics and Physics Solids*, Vol. 9, July 1961, p. 152.
- ⁷Zienkiewicz, O. C., *The Finite Element Method in Engineering Science*, McGraw-Hill, London, 1971.
- ⁸Rosen, W. B. and Dow, N. F., "Evaluations of Filament-Reinforced Composites for Aerospace Structural Applications," NASA CR-207, General Electric Co., Philadelphia, Pa., p. 123.
- ⁹Casalengo, L., Martini, G., and Ruspa, G., "Uses of Models to Estimate Fuselage Pressure in VTOL Aircraft," *Journal of Sound and Vibration*, Vol. 17, Aug. 1971, p. 309.
- ¹⁰Chapman, A. J., *Heat Transfer*, 2nd ed., Macmillan, New York, 1967, p. 330.

From the AIAA Progress in Astronautics and Aeronautics Series . . .

AEROACOUSTICS: FAN, STOL, AND BOUNDARY LAYER NOISE; SONIC BOOM; AEROACOUSTIC INSTRUMENTATION—v. 38

Edited by Henry T. Nagamatsu, General Electric Research and Development Center; Jack V. O'Keefe, The Boeing Company; and Ira R. Schwartz, NASA Ames Development Center

A companion to Aeroacoustics: Jet and Combustion Noise; Duct Acoustics, volume 37 in the series.

Twenty-nine papers, with summaries of panel discussions, comprise this volume, covering fan noise, STOL and rotor noise, acoustics of boundary layers and structural response, broadband noise generation, airfoil-wake interactions, blade spacing, supersonic fans, and inlet geometry. Studies of STOL and rotor noise cover mechanisms and prediction, suppression, spectral trends, and an engine-over-the-wing concept. Structural phenomena include panel response, high-temperature fatigue, and reentry vehicle loads, and boundary layer studies examine attached and separated turbulent pressure fluctuations, supersonic and hypersonic.

Sonic boom studies examine high-altitude overpressure, space shuttle boom, a low-boom supersonic transport, shock wave distortion, nonlinear acoustics, and far-field effects. Instrumentation includes directional microphone, jet flow source location, various sensors, shear flow measurement, laser velocimeters, and comparisons of wind tunnel and flight test data.

509 pp. 6 x 9, illus. \$19.00 Mem. \$30.00 List

TO ORDER WRITE: Publications Dept., AIAA, 1290 Avenue of the Americas, New York, N. Y. 10019